Singular solutions, momentum maps and computational anatomy

Colin J. Cotter, Darryl D. Holm

Singular solutions, momentum maps and computational anatomy

Colin J. Cotter[1] and Darryl D. Holm[1,2]

[1] Department of Mathematics, Imperial College London, SW7 2AZ, UK
colin.cotter@imperial.ac.uk
[2] Los Alamos National Laboratory, Los Alamos, NM 87545 USA
d.holm@imperial.ac.uk, dholm@lanl.gov

Abstract. This paper describes the variational formulation of template matching problems of computational anatomy (CA); introduces the EPDiff evolution equation in the context of an analogy between CA and fluid dynamics; discusses the singular solutions for the EPDiff equation and explains why these singular solutions exist (singular momentum map). Then it draws the consequences of EPDiff for outline matching problem in CA and gives numerical examples.

"I shall speak of things . . . so singular in their oddity as in some manner to instruct, or at least entertain, without wearying." – Lorenzo da Ponte

1 Introduction

Computational Anatomy (CA) must measure and analyze a range of variations in shape, or appearance, of highly deformable structures. The problem statement for CA was formulated long ago [1]

> In a very large part of morphology, our essential task lies in the ***comparison of related forms*** rather than in the precise definition of each. . . . This process of comparison, of recognizing in one form a definite permutation or deformation of another, . . . lies within the immediate province of mathematics and finds its solution in . . . the Theory of Transformations. – D'Arcy Thompson, *On Growth and Form* (1917)

The pioneering work of Bookstein, Grenander and Bajscy [2–4] first took up this challenge by introducing a method called template matching. The past several years have seen an explosion in the use of template matching methods in computer vision and medical imaging that is fulfilling D'Arcy Thompson's expectation [5–19]. These methods enable the systematic measurement and comparison of anatomical shapes and structures in medical imagery. The mathematical theory of Grenander's deformable template models, when applied to these problems, involves smooth invertible maps (diffeomorphisms), as presented in this context in [9, 10, 18–21]. In particular, the template matching approach involves Riemannian metrics on the diffeomorphism group and employs their projections onto specific landmark shapes, or image spaces.

The problem for CA then becomes to minimize the distance between two images as specified in a certain representation space, V. Metrics are written so that the optimal path in V satisfies an evolution equation, which was first discovered in abstract form [22] and later called EPDiff when it arose in the Euler-Poincaré theory of optimal motion on smooth invertible mappings called diffeomorphisms, [23].

The EPDiff equation coincides with the Euler equation for ideal fluids in the case that the Riemannian metric for the distance between two images is the L^2 norm. Another type of norm on V (called the H^1 norm) arises in the theory of the fascinating nonlinear coherent solutions of shallow water waves called ***solitons***. Solitons interact with each other elastically, so they re-emerge unscathed from fully nonlinear collisions. EPDiff with the H^1 norm on V describes the peaked soliton solutions of the Camassa-Holm shallow water wave equation. As we shall see, the Camassa-Holm peakons arise from a general property of Hamiltonian systems called their ***momentum map***. A discussion of EPDiff and peakons in the particular case of template matching appears in [24].

In this paper, we shall draw parallels between the two endeavors of fluid dynamics and template matching for computational anatomy, by showing how the Euler-Poincaré theory of ideal fluids can be used to develop new perspectives in CA. In particular, we discover that CA may be informed by the concept of weak solutions, solitons and momentum maps for geodesic flows [24–26].

1.1 Problem & Approach for Computational Anatomy

Computational Anatomy (CA) compares shapes (graphical structures) by making a ***geodesic deformation*** from one shape to the another. Among these graphical structures, landmarks and image outlines in CA are found to be singular solutions of the geodesic ***EPDiff*** equation. A ***momentum map*** for singular solutions of EPDiff yields their canonical Hamiltonian formulation, which provides a ***complete parameterization*** of the landmarks and image outlines by their ***canonical positions and momenta***. The momentum map provides an ***isomorphism*** between landmarks (and outlines) for images and ***singular*** (weak) solutions of EPDiff. (These solutions are solitons in 1D.) This isomorphism provides for CA: (1) a complete and non-redundant data representation; (2) a dynamical paradigm in which image outlines interact by exchange of momentum; (3) methods for numerical simulation & data assimilation. Euler-Poincaré theory also provides a framework for unifying and extending the various approaches in CA.

Thus, the concept of momentum becomes important for CA, because momentum:
– Completes the representation of images (momentum of cartoons);
– Informs template matching of the possibility of soliton-like collisions and ***momentum exchange in image outline interactions***;
– Encodes the subsequent deformation into the ***initial locus and momentum*** of an image outline;
– Provides numerical simulation methods using the ***momentum map for***

right action as a data structure; and
– Accomplishes matching and data assimilation via the ***adjoint linear problem*** for template matching, using the ***initial momentum as a control variable***.
All of these momentum properties flow from the ***EPDiff*** equation.

Outline of the paper. Section 2 describes the template matching variational problems of computational anatomy, explains the analogy with fluid dynamics and introduces the fundamental EPDiff evolution equation. The singular solutions for the EPDiff equation (2.1) with diffeomorphism group G are discussed in section 3. They are, in particular, related to the outline matching problem in computer vision, examples of which are given in section 4.

2 Mathematical formulation of template matching for CA

2.1 Cost

Most problems in CA can be formulated as: ***Find the deformation path (flow) with minimal cost, under the constraint that it carries the template to the target***. Such problems have a remarkable analogy with fluid dynamics. The ***cost*** assigned in template matching for comparing images $\mathcal{I}_0$ & $\mathcal{I}_1$ is specified as a functional

$$\text{Cost}(t \mapsto \varphi_t) = \int_0^1 \ell(\mathbf{u}_t)\, dt$$

defined on curves φ_t in a Lie group with tangents $\frac{d\varphi_t}{dt} = \mathbf{u}_t \circ \varphi_t$ and $\mathcal{I}_t = \varphi_t \cdot \mathcal{I}_0$. In what follows, the function $\mathbf{u}_t \mapsto \ell(\mathbf{u}_t) = \|\mathbf{u}_t\|^2$ will be taken as a squared functional norm on the space of velocity vectors along the flow. The Lie group property specifies the representation space for template matching as a manifold of smooth mappings, which may be differentiated, composed and inverted. The vector space of ***right invariant*** instantaneous velocities, $\mathbf{u}_t = (d\varphi_t/dt) \circ \varphi_t^{-1}$ forms the tangent space at the identity of the considered Lie group, and may be identified as the group's ***Lie algebra***, denoted $\mathfrak{g}$.

2.2 Mathematical analogy between template matching and fluid dynamics

(I) The frameworks of CA and fluid dynamics both involve a ***right-invariant*** stationary principle with action, or cost function. The main differences are that template matching is formulated as an optimal control problem whose cost function is designed for the application, while fluid dynamics is formulated as an initial value problem whose cost function is the fluid's kinetic energy.
(II) The geodesic evolution for both template matching and fluid dynamics is governed by the ***EPDiff equation*** [27, 21],

$$\Big(\frac{\partial}{\partial t} + \mathbf{u}\cdot\nabla\Big)\mathbf{m} + (\nabla\mathbf{u})^T\cdot\mathbf{m} + \mathbf{m}(\text{div}\,\mathbf{u}) = 0\,. \tag{2.1}$$

Here $\mathbf{u} = G * \mathbf{m}$, where $G*$ denotes convolution with the Green's kernel G for the operator Q_{op}, where

$$\mathbf{m} = \frac{\delta \ell}{\delta \mathbf{u}} =: Q_{op}\mathbf{u}$$

The operator Q_{op} is symmetric and positive definite for the cost defined by

$$\text{Cost}(t \mapsto \varphi_t) = \int_0^1 \ell(\mathbf{u}_t)\, dt = \frac{1}{2}\int_0^1 \|\mathbf{u}_t\|^2\, dt = \frac{1}{2}\int_0^1 \langle\, \mathbf{u}_t\,,\, Q_{op}\mathbf{u}_t\,\rangle\, dt$$

with L^2 pairing $\langle\, \cdot\,,\, \cdot\,\rangle$ whenever $\|\mathbf{u}_t\|^2$ is a norm.
(III) The flows in CA and fluid dynamics both evolve under a left group action on a linear representation space, $\mathcal{I}_t = \varphi_t \cdot \mathcal{I}_0$. They differ in the roles of their advected quantities, $a_t = a_0 \circ \varphi_t^{-1}$. The main difference is that image properties are passive and affect the template matching as a constraint in the cost function, while advected quantities may affect fluid flows directly, for example through the pressure, so as to produce waves.

2.3 How EPDiff emerges in CA

Choose the cost function for continuously morphing $\mathcal{I}_0$ into $\mathcal{I}_1$ as

$$\text{Cost}(t \mapsto \varphi_t) = \int_0^1 \ell(\mathbf{u}_t)\, dt = \int_0^1 \|\mathbf{u}_t\|^2\, dt\,,$$

where u_t is the velocity of the fluid deformation at time t and

$$\|\mathbf{u}_t\|^2 = \langle\, \mathbf{u}_t\,,\, Q_{op}\mathbf{u}_t\,\rangle\,,$$

and Q_{op} is our positive symmetric linear operator. Then, the momentum governing the process, $\mathbf{m}_t = Q_{op}\mathbf{u}_t$ with Green's function $G:\ \mathbf{u}_t = G * \mathbf{m}_t$ satisfies the EPDiff equation, (2.1). This equation arises in both template matching and fluid dynamics, and it informs both fields of endeavor.

2.4 Deriving EPDiff from Euler-Poincaré Reduction of Hamilton's principle

.

Euler-Poincaré Reduction starts with a right (or left) $G-$invariant Lagrangian $L : TG \to \mathbb{R}$ on the tangent bundle of a Lie group G. ***Right invariance*** of the Lagrangian may be written as

$$L(g(t), \dot{g}(t)) = L(g(t)h, \dot{g}(t)h)\,,\ \text{for all } h \in G$$

A $G-$invariant Lagrangian defined on TG possesses a symmetry-reduced Hamilton's principle defined on the Lie algebra $TG/G \simeq \mathfrak{g}$. Stationarity of the symmetry-reduced Hamilton's principle yields the ***Euler-Poincaré equations*** on the dual Lie algebra $\mathfrak{g}^*$. For $G = \text{Diff}$, this equation is ***EPDiff*** (2.1).

3 Outline matching & momentum measures

Problem statement for outline matching:
Given two collections of curves $c_1, \ldots, c_N$ and $C_1, \ldots, C_N$ in Ω, find a time-dependent diffeomorphic process $(t \mapsto \varphi_t)$ of minimal action (or cost) such that $\varphi_0 = \mathrm{id}$ and $\varphi_1(c_i) = C_i$ for $i = 1, \ldots, N$. The matching problem for the image outlines seeks ***singular momentum solutions*** which naturally emerge in the computation of geodesics.

3.1 Image outlines as Singular Momentum Solutions of EPDiff

For example, in the 2D plane, EPDiff has weak ***singular momentum solutions*** that are expressed as [25, 23, 26]

$$\mathbf{m}(\mathbf{x}, t) = \sum_{a=1}^{N} \int_s \mathbf{P}_a(t, s)\delta\big(\mathbf{x} - \mathbf{Q}_a(t, s)\big)\, ds\,, \tag{3.1}$$

where s is a ***Lagrangian coordinate*** defined along a set of N curves in the plane *moving with the flow* by the equations $\mathbf{x} = \mathbf{Q}_a(t, s)$ and supported on the delta functions in the EPDiff solution (3.1). Thus, the singular momentum solutions of EPDiff represent evolving "wavefronts" supported on delta functions defined along curves $\mathbf{Q}_a(t, s)$ with arclength coordinate s and carrying momentum $\mathbf{P}_a(t, s)$ at each point along the curve as specified by (3.1). These solutions exist in any dimension and they provide a means of performing CA matching for points (landmarks), curves and surfaces, in any combination.

3.2 Here is the Geometry – Leading to the Numerics

The basic observation that ties everything together in $n-$dimensions is the following:
Theorem (Holm and Marsden, [23]): EPDiff singular momentum solutions $T^*\mathrm{Emb}(S, \mathbb{R}^n) \to \mathfrak{g}^* :\ (\mathbf{P}, \mathbf{Q}) \to \mathbf{m}$ ***define a momentum map.***

It is beyond our scope here to explain either the proof of this theorem or the mathematics underlying momentum maps for diffeomorphisms. However, we summarize the main results for template matching, as follows:
– The embedded manifold S is the support set of the P's and Q's.
– The momentum map is for left action of the diffeomorphisms on S.
– The whole system is right invariant.
– Consequently, its momentum map for right action is conserved.
– These constructions persist for a certain class of numerical schemes.
– They apply in template matching for every choice of norm.

3.3 A familiar example of a momentum map

A ***momentum map*** $\mathbf{J} : T^*Q \mapsto \mathfrak{g}^*$ is a Hamiltonian for the canonical action of a Lie group G on phase space T^*Q. It is expressed in terms of the pairing

$\langle \cdot\,, \cdot \rangle : \mathfrak{g}^* \times \mathfrak{g} \mapsto \mathbb{R}$ as

$$\langle \mathbf{J}\,, \xi \rangle = \langle p\,,\, \pounds_\xi q \rangle =: \langle q \diamond p\,, \xi \rangle\,,$$

where $(q, p) \in T^*_q Q$ and the Lie derivative $\pounds_\xi q$ is the infinitesimal generator of the action of the Lie algebra element $\xi \in \mathfrak{g}$ on q in the manifold Q.

The standard example is $\pounds_\xi q = \xi \times q$ for $\mathbb{R}^3 \times \mathbb{R}^3 \mapsto \mathbb{R}^3$, with pairing $\langle \cdot\,, \cdot \rangle$ given by scalar product of vectors. The momentum map is then

$$\mathbf{J} \cdot \xi = p \cdot \xi \times q = q \times p \cdot \xi \Rightarrow \mathbf{J} = q \times p$$

This is ***angular momentum***, the Hamiltonian for phase-space rotations. The outlines of images may be parameterized as curves whose dynamics must be invariant under reparameterizing the arclengths that label those curves. This symmetry leads to a conserved momentum map, called the ***circulation*** along the curves. The analog of this conservation law for fluids is the classical Kelvin circulation theorem.

3.4 EPDiff dynamics informs optimal control for CA

CA must compare two geometric objects, and thus it is concerned with an ***optimal control problem***. However, the ***initial value problem*** for EPDiff also has ***important consequences for CA applications***.

- When matching two geometric structures, the ***momentum at time*** *t=0* ***contains all required information for reconstructing the target from the template***. This is done via ***Hamiltonian geodesic flow***.
- Being canonically conjugate, the momentum has exactly the same dimension as the matched structures, so there is ***no redundancy***.
- Right invariance mods out the relabeling motions from the optimal solution. This symmetry also yields a ***conserved momentum map***.
- Besides being one-to-one, the momentum representation is defined on a ***linear space***, being dual to the velocity vectors.

  This means one may, for example,:
  - study linear instability of CA processes,
  - take averages and
  - apply statistics to the space of image contours.

  The ***advantage*** is the ease of building, sampling and estimating statistical models on a ***linear space***.

3.5 Summary

We have identified ***momentum as a key concept*** in the representation of image data for CA and discussed analogies with fluid dynamics. The ***fundamental idea*** transferring from fluid dynamics to CA is the idea of ***momentum maps*** corresponding to group actions.

4 Numerical examples of outline matching

In this section we describe our new technique applying particle-mesh methods to the problem of matching outlines. First we describe the approach to calculating geodesics in the space of outlines.

Let $\boldsymbol{Q}_0$ and $\boldsymbol{Q}_1$ be two embeddings of S^1 in $\mathbb{R}^2$ which represent two shapes, each a closed planar curve. We seek a 1-parameter family of embeddings $\boldsymbol{Q}(t) : S^1 \times [0,1] \to \mathbb{R}^2$ so that $\boldsymbol{Q}(0) = \boldsymbol{Q}_0$ and $\boldsymbol{Q}(1)$ matches $\boldsymbol{Q}_1$ (up to relabeling). $\boldsymbol{Q}(t)$ is found by minimizing the constrained norm of its velocity. To find the equation for $\boldsymbol{Q}$ we require extremal values of the action

$$A = \int_0^1 \frac{1}{2} L(\boldsymbol{u}) \,\mathrm{d}\, t + \int_0^1 \int_{S^1} \boldsymbol{P}(s,t) \cdot (\dot{\boldsymbol{Q}}(s,t) - \boldsymbol{u}(\boldsymbol{Q}(s,t))) \,\mathrm{d}\, t, \qquad L = \|\boldsymbol{u}(t)\|^2_{\mathfrak{g}},$$

i.e. we seek time-series of vector fields $\boldsymbol{u}(t)$ which are minimized in some norm subject to the constraint that $\boldsymbol{Q}$ is advected by the flow using the Lagrange multipliers $\boldsymbol{P}$ (which we call momentum). The minimizing solutions are

$$\frac{\delta L}{\delta \boldsymbol{u}} = \int_{S^1} \boldsymbol{P}(s,t) \delta(\boldsymbol{x} - \boldsymbol{Q}(s,t)) \,\mathrm{d}\, s, \tag{4.1}$$

$$\dot{\boldsymbol{P}}(s,t) = -\boldsymbol{P}(s,t) \cdot \nabla \boldsymbol{u}(\boldsymbol{Q}(s,t),t), \tag{4.2}$$

$$\dot{\boldsymbol{Q}}(s,t) = \boldsymbol{u}(\boldsymbol{Q}(s,t),t), \tag{4.3}$$

subject to $\boldsymbol{Q}(s,0) = \boldsymbol{Q}_0(s)$.

We note that equation (4.1) is the momentum map corresponding to the cotangent-lift of the action of vector fields $\boldsymbol{u}$ on embedded curves given by

$$\boldsymbol{Q} \mapsto \boldsymbol{u}(\boldsymbol{Q}).$$

For a suitable test function $\boldsymbol{w}$, we obtain

$$\frac{d}{dt}\langle \boldsymbol{w}, \boldsymbol{m} \rangle - \langle \nabla \boldsymbol{w}, \boldsymbol{u}\boldsymbol{m} \rangle + \langle \boldsymbol{w}, (\nabla \boldsymbol{u})^T \cdot \boldsymbol{m} \rangle = 0, \qquad \boldsymbol{m} = \frac{\delta L}{\delta \boldsymbol{u}},$$

which is the weak form of the EPDiff equation.

Now one must seek initial momentum $\boldsymbol{P}(s,0)$ which takes shape $\boldsymbol{Q}_0(s)$ to shape $\boldsymbol{Q}_1(s)$. To do this, we choose some functional J of the advected shape $\boldsymbol{Q}(1,s)$ which is minimized when $\boldsymbol{Q}(1,s)$ matches $\boldsymbol{Q}_1(s)$. Following [28], we describe the curves by singular densities:

$$\mu = \int_{S_1} \hat{\mu}(s) \delta(\boldsymbol{x} - \boldsymbol{Q}(1,s) \,\mathrm{d}\, s \,\mathrm{d}\, V(\boldsymbol{x}), \tag{4.4}$$

$$\eta = \int_{S_1} \hat{\eta}(s) \delta(\boldsymbol{x} - \boldsymbol{Q}_1(s) \,\mathrm{d}\, s \,\mathrm{d}\, V(\boldsymbol{x}), \tag{4.5}$$

and write $J = \|\mu - \eta\|^2_G$ where $\|\cdot\|^2_G$ is a norm for a densities in a reproducing kernel Hilbert space with kernel G. This approach means that we do not need to force particular points to be matched to each other on the shapes. This last problem can be solved by using a gradient algorithm, where the gradient of the residual error with respect to $\boldsymbol{P}(s,0)$ is calculated using the adjoint equation [29].

4.1 Numerical discretization

We use the Variational Particle-Mesh (VPM) method [30, 31] to discretize the equations (4.1-4.3), as follows: discretize the velocity on an Eulerian grid with n_g points and approximate $\|\boldsymbol{u}\|$ there; replace S^1 by representing the shape by a finite set of n_p Lagrangian particles $\{\boldsymbol{Q}_\beta\}_{\beta=1}^{n_p}$, and interpolate from the grid to the particles using basis functions

$$\boldsymbol{u}(\boldsymbol{Q}_\beta) = \sum_{k=1}^{n_g} \boldsymbol{u}_k \psi_k(\boldsymbol{Q}_\beta)\,, \quad \text{with} \quad \sum_{k=1}^{n_g} \psi_k(\boldsymbol{x}) = 1\,,\ \forall\ \boldsymbol{x}.$$

The action for the continuous time motion on the grid then becomes

$$A = \int_0^1 \frac{1}{2}\|\boldsymbol{u}(t)\|_{grid}^2 + \sum_\beta \boldsymbol{P}_\beta \cdot \left(\dot{\boldsymbol{Q}}_\beta - \sum_k \boldsymbol{u}_k \psi_k(\boldsymbol{Q}_\beta)\right) \mathrm{d}\, t,$$

and one can obtain a fully discrete method by discretizing the action in time. For example, we can obtain a first-order method by extremizing

$$A = \Delta t \sum_{n=1}^{N} \left(\frac{1}{2}\|\boldsymbol{u}^n\|_{grid}^2 + \sum_\beta \boldsymbol{P}_\beta^n \cdot \left(\frac{\boldsymbol{Q}_\beta^n - \boldsymbol{Q}_\beta^{n-1}}{\Delta t} - \sum_k \boldsymbol{u}_k^n \psi_k(\boldsymbol{Q}_\beta^{n-1}) \right) \right).$$

The resulting time-stepping method is the (first-order) symplectic Euler-A method for the time-continuous Hamiltonian system for the Lagrangian particles. In general, the method will always be symplectic since it arises from a discrete variational principle (see [32] for a broad introduction to symplectic numerical methods and their conservation properties). The conservation properties of VPM are discussed in [31].

We approximate the densities μ and η on the grid using the standard particle-mesh approach (see [33]):

$$\mu_k = \sum_\beta \hat{\mu}_\beta \psi_k(\boldsymbol{Q}_\beta^N), \qquad \eta_k = \sum_\beta \hat{\eta}_\beta \psi_k(\boldsymbol{Q}_{1,\beta}),$$

where $\boldsymbol{Q}_{1,\beta}$ are the positions of particles on the target shape. This amounts to "pixellating" the singular densities (4.4-4.5) on the grid. For a given kernel G, we approximate J with

$$J = \sum_{kl} G(\boldsymbol{x}_k - \boldsymbol{x}_l)(\mu_k - \eta_k)(\mu_l - \eta_l).$$

The discrete adjoint is then applied in computing the inversion for the initial conditions for $\boldsymbol{P}_\beta$ which generate the flow. A numerical example calculated using this method is given in figure 1.

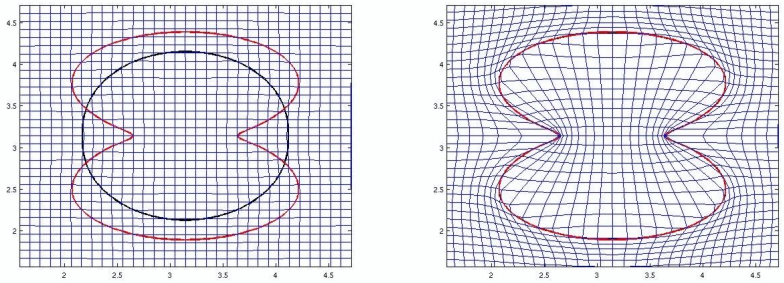

Fig. 1. Results from a VPM calculation to calculate the minimal path between a two simple shapes. On the left, the initial and final shapes are shown, and on the right, the deformation of the initial shape into the final shape is depicted together with a grid which shows how the flow map deforms the space around the shape. We used the H^1 norm for velocity on a $2\pi \times 2\pi$ periodic domain on a 128×128 grid, discretized using FFT, and the corresponding kernel was used to calculate J. Cubic B-splines were used as basis functions.

Conclusion

We have presented the formulation and numerical implementation of D'Arcy Thompson's vision of how transformation theory would provide a natural means of anatomical comparison, of recognizing shape and form. For this, we have identified momentum as a key concept in the representation of image data for CA and have discussed the analogies of CA with fluid dynamics. The fundamental idea that transfers from fluid dynamics to CA is the idea of momentum maps corresponding to group actions. The analogy of CA with fluid dynamics also suggests that much remains to be gained by understanding modern methods in fluid dynamics and seeking ways to transfer these ideas to CA.

In addition, we have illustrated the power of this method by solving a simple but challenging problem of exact matching of two closed contours in the plane. This example is deceptively simple looking, in fact the computation of exact matching had never been done before and is still a challenging problem for computational anatomy.

Acknowledgments

This work was partially supported by US DOE, under contract W-7405-ENG-36 for Los Alamos National Laboratory, and Office of Science ASCAR/AMS/MICS.

References

1. Thompson, D.: On Growth and Form. (1917)

2. Bajcsy, R., Lieberson, R., Reivich, M.: A computerized system for the elastic matching of deformed radiographic images to idealized atlas images. J. Comput. Assisted Tomogr. **7** (1983) 618–625
3. Bookstein, F.L.: Morphometric tools for landmark data; geometry and biology. Cambridge University press (1991)
4. Grenander, U.: General Pattern Theory. Oxford Science Publications (1993)
5. Ashburner, J., Csernansky, J.G., Davatzikos, C., Fox, N.C., Frisoni, G.B., Thompson, P.M.: Computer-assisted imaging to assess brain structure in healthy and diseased brains. Lancet Neurology **2** (2003) 79–88
6. Grenander, U., Miller, M.I.: Computational anatomy: An emerging discipline. Quarterly of Applied Mathematics **LVI**(4) (1998) 617–694
7. Hallinan, P.: A low dimensional model for face recognition under arbitrary lighting conditions. In: Proceedings CVPR'94. (1994) 995–999
8. Jain, A.K., Zhong, Y., Dubuisson-Jolly, M.P.: Deformable template models: a review. Signal Processing **71** (1998) 109–129
9. Miller, M.I., Trouvé, A., Younes, L.: On metrics and Euler-Lagrange equations of computational anatomy. Ann. Rev. Biomed. Engng **4** (2002) 375–405
10. Miller, M.I., Younes, L.: Group action, diffeomorphism and matching: a general framework. Int. J. Comp. Vis. **41** (2001) 61–84
11. Montagnat, J., Delingette, H., Ayache, N.: A review of deformable surfaces: topology, geometry and deformation. Image and Vision Computing **19** (2001) 1023–1040
12. Mumford, D.: Mathematical theories of shape: Do they model perception ? In: Proc. SPIE Workshop on Geometric Methods in Computer Vision. Volume 1570. SPIE, Bellingham, WA (1991) 2–10
13. Mumford, D.: Elastica and computer vision. In: Algebraic Geometry and its Applications. Springer-Verlag, New York, NY (1994) 507–518
14. Mumford, D.: Pattern theory: a unifying perspective. In: Perception as Bayesian Inference. Cambridge University Press, Cambridge, UK (1996) 25–62
15. Thompson, P.M., Giedd, J.N., Woods, R.P., MacDonald, D., Evans, A.C., Toga, A.W.: Growth patterns in the developing brain detected by using continuum mechanical tensor maps. Nature **404**(6774) (2000) 190–3.
16. Toga, A.W., ed.: Brain warping. Academic Press (1999)
17. Toga, A.W., Thompson, P.M.: Temporal dynamics of brain anatomy. Ann. Rev. Biomedical Engng. **5** (2003) 119–145
18. Trouvé, A.: An infinite dimensional group approach for physics based model. Technical report (electronically available at http://www.cis.jhu.edu) (1995)
19. Trouvé, A.: Diffeomorphism groups and pattern matching in image analysis. Int. J. of Comp. Vis. **28**(3) (1998) 213–221
20. Dupuis, P., Grenander, U., Miller, M.I.: Variational problems on flows of diffeomorphisms for image matching. Quarterly of Applied Math. **56** (1998) 587–600
21. Mumford, D.: Pattern theory and vision. In: Questions Mathmatiques En Traitement Du Signal et de L'Image. Institut Henri Poincar (1998) 7–13
22. Arnold, V.I.: Mathematical methods of Classical Mechanics. Springer (1978) Second Edition: 1989.
23. Holm, D.D., Marsden, J.E.: Momentum maps & measure valued solutions of the Euler-Poincar equations for the diffeomorphism group. Progr. Math. **232** (2004) 203–235 http://arxiv.org/abs/nlin.CD/0312048.
24. Holm, D.D., Rananather, J.T., Trouvé, A., Younes, L.: Soliton dynamics in computational anatomy. NeuroImage **23** (2004) S170–178 http://arxiv.org/abs/nlin.SI/0411014.

25. Camassa, R., Holm, D.D.: An integrable shallow water equation with peaked solitons. Phys. Rev. Lett. **71** (1993) 1661–1664
26. Holm, D.D., Staley, M.F.: Interaction dynamics of singular wavefronts in nonlinear evolutionary fluid equations. Technical report, Los Alamos National Laboratory (2004) In preparation, see http://cnls.lanl.gov/ staley/.
27. Holm, D.D., Marsden, J.E., Ratiu, T.S.: The Euler–Poincar equations and semidirect products with applications to continuum theories. Adv. in Math. **137** (1998) 1–81 http://xxx.lanl.gov/abs/chao-dyn/9801015.
28. Glaunes, J., Trouve, A., Younes, L.: Diffeomorphic matching of distributions: A new approach for unlabelled point-sets and sub-manifolds matching. In: IEEE Computer Society Conference on Computer Vision and Pattern Recognition. Volume 2. (2004) 712–718
29. Gunzburger, M.D.: Perspectives in Flow Control and Optimization. Advances in design and control. SIAM, Philadelphia, USA (2003)
30. Cotter, C.J.: A general approach for producing Hamiltonian numerical schemes for fluid equations. arXiv:math.NA/0501468 (2005)
31. Cotter, C.J., Holm, D.D.: Discrete momentum maps for lattice EPDiff. arXiv:math.NA/0602296 (2006)
32. Leimkuhler, B., Reich, S.: Simulating Hamiltonian Dynamics. CUP (2005)
33. Frank, J., Gottwald, G., Reich, S.: A Hamiltonian particle-mesh method for the rotating shallow-water equations. In: Lecture Notes in Computational Science and Engineering. Volume 26. Springer-Verlag (2002) 131–142